Düzce University Journal of Science & Technology, 12(2024) 1913-1929

Düzce University
Journal of Science & Technology

Research Article

Drying of Nettle Using Concentrated Air Collector and Concentrated Photovoltaic Thermal Supported Drying System and Modeling with Machine Learning

Mehmet Onur KARAAĞAÇ [a,b] *

[a] *Department of Energy Systems Engineering, Faculty of Engineering and Architecture, Sinop University, Sinop, TÜRKİYE*
[b] *Energy Research and Application Center, Sinop University, Sinop, TÜRKİYE*
* *Corresponding author's e-mail address: okaraagac@sinop.edu.tr*
DOI: 10.29130/dubited.1460576

ABSTRACT

This study examines the performance of a solar assisted drying system in the nettle drying process. The drying process works by using thermal energy obtained from solar air collectors and PV modules. The experimental were carried out in October 2022, and the room temperature, total efficiency and moisture content parameters were investigated. The data obtained from the drying system were modelled using machine learning algorithms such as artificial neural networks (ANN), support vector machines (SVM), and gradient boosting decision trees (GBDT). The average thermal energy transferred to the drying cabin was calculated as 154 W, with 77% of this energy was obtained from the air collector and the remaining 23% from the PV module. The stinging nettle was dried from an initial moisture content of 11.18 g water/g dry matter to a final moisture content of 1.18 g water/g dry matter. The average total efficiency of the drying system was found to be 16.8%. Additionally, the results show that the SVM algorithm exhibits the best performance in estimating important parameters such as chamber temperature, moisture content, and total efficiency. Especially in total efficiency prediction. The SVM algorithm has a significant advantage over other algorithms. As a result, it was concluded that the SVM algorithm can be used effectively utilized in solar energy-supported drying systems and can be a precious choice for the optimization of the drying process.

Keywords: *Solar energy-supported drying systems, Machine learning algorithms, Drying process optimization*

Yoğunlaştırılmış Havalı Kolektör ve Yoğunlaştırılmış Fotovoltaik Termal Destekli Bir Kurutma Sistemi ile Isırgan Otunun Kurutulması ve Sistem Verilerinin Makine Öğrenmesi ile Modellenmesi

ÖZ

Bu çalışma, ısırgan otu kurutma sürecinde güneş enerjisi destekli bir kurutma sisteminin performansını incelemektedir. Kurutma işlemi, havalı güneş kolektöründen ve PV modüllerden elde edilen termal enerjiyi kullanarak çalışmaktadır. Deneyler, 2022 yılı ekim ayında gerçekleştirilmiş ve oda sıcaklığı, toplam verimlilik ve nem içeriği parametrelerin değişimi incelenmiştir. Kurutma sürecinde elde edilen veriler, yapay sinir ağı (YSA), destek vektör makinesi (SVM) ve gradyan artırıcı karar ağacı (GBDT) gibi makine öğrenmesi algoritmaları kullanılarak modellenmiştir. Isırgan otu başlangıçta 11,18 gr su / gr kuru madde nem içerirken, 1,18 gr su /gr kuru madde miktarına kadar kurutulmuştur. Kurutma kabinine aktarılan ortalama termal enerji 154 W olarak hesaplanmıştır. Bu enerjinin %77 kolektörden geri kalan %23 kısımda FV modelden elde edilmiştir. Kurutma sisteminin ortalama toplam verimi %16,8 olarak hesaplanmıştır. Isırgan otu başlangıçta 11,18 gr su / gr kuru madde nem içeriğinden 1,18 gr su /gr kuru madde miktarına kadar kurutulmuştur. Ayrıca elde edilen sonuçlar, kabin

Received: 28/03/2024, Revised: 05/04/2024, Accepted: 23/05/2024

sıcaklığı, nem içeriği ve toplam verim gibi önemli parametrelerin tahmin edilmesinde SVM algoritmasının en iyi performansı sergilediğini göstermektedir. Özellikle toplam verim tahmininde SVM algoritması, diğer algoritmalara göre önemli bir üstünlük sağlamıştır. Sonuç olarak, güneş enerjisi destekli kurutma sistemlerinde SVM algoritmasının etkili bir şekilde kullanılabileceği ve kurutma sürecinin optimize edilmesinde değerli bir araç olabileceği sonucuna varılmıştır.

Anahtar Kelimeler: *Güneş enerjisi destekli kurutma sistemleri, Makine öğrenme algoritmaları, Kurutma prosesi optimizasyonu*

Nomenclature

A	Area (m^2)
ANN	Artificial Neural Networks
Cp	Specific heat (kJ/(kg K))
GBDT	Gradient Boosting Decision Trees
GPR	Gaussian Process Regression
LM	Levenberg-Marquardt
ML	Machine Learning
MAPE	Mean Absolute Percentage Error
PTSC	Parabolic Trough Solar Collectors
RSM	Response Surface Methodology
RMSE	Root Mean Square Error
R^2	Coefficients Of Determination
SVM	Support Vector Machines
SAC	Solar Air Collector
I(t)	Solar radiation (W/m2)
L	Latent heat (kJ/kg)
m	Mass (kg)
PV	Photovoltaic
PV/T	Photovoltaic-thermal
T	Temperature (°C)
Q	Thermal energy (kJ)
W	Electrical energy input (kJ)

Subscripts

a	Ambient
i	Initial
in	Inlet
L	Liquid
out	Outlet
w	water

I. INTRODUCTION

Considering that Türkiye is in an extremely advantageous position, especially in terms of solar energy, the use of this resource is of much greater importance than industrial and critical importance. The increasing energy demand and limited fossil fuel reserves have led humanity to search for different energy sources. As a result of studies and research, many new approaches have been developed for heat energy and electricity production using solar energy, a renewable energy source. The solar energy usage has become extensive in many areas such as heating, cooling, and air conditioning systems [1], [2], [3], electricity production [4], [5], clean water production [6], agricultural areas [7], [8], and drying of products [9], [10], [11], [12].

Solar energy-supported drying systems are emerging as an environmentally friendly and sustainable option for drying agricultural products. These systems include solar air collectors, PV panels, and air circulation systems to dry products using solar. Drying products with high water content can reduce energy costs and minimize environmental impact using renewable energy sources. Drying agricultural and industrial products under the sun has been used since ancient times. However, this method lacks control over the drying process and cannot provide a hygienic environment against environmental effects such as rain and dust. Therefore, it is important to use closed systems where the process is controlled and homogeneous drying is ensured, instead of drying under the sun [13]. Traditional drying systems require the development of new systems and methods due to high electricity costs.

Concentrated solar energy drying of agricultural and industrial products is widely utilized, aiming to minimize energy consumption by eliminating disadvantages encountered in sun drying and traditional methods. Enclosed cabinet solar-powered drying systems offer advantages over sun drying systems, including protection of the product against pollutants and pests, reduction of external factors such as rain, ensuring homogeneous temperature and humidity distribution, and control over the desired temperature level. Among solar energy-supported drying systems, air collector dryers with solar collectors are the most prevalent. These systems consist of a solar-powered air collector, a circulation fan, and a drying chamber. A typical solar-powered air collector comprises an absorber plate, parallel plates through which air flows, a glass or plastic covering at the top, and an insulated casing at the bottom and sides [14]. Despite being produced in various designs, solar-powered air collectors operate on the same principle. Plates with different surface profiles serving as absorbers are stacked with gaps in between, allowing air passing through the gaps to absorb heat upon contact with the absorber surface. As a result of this contact, the air exits the collector as hot air. Numerous significant studies concerning solar energy-supported systems for agricultural and industrial product drying exist. Some studies related to hot air production, product drying systems, and convective heat transfer could be found below.

Uçar and Oral conducted an experimental analysis of a cabin heating system using a solar air collector (SAC). This system employed two SACs with solar energy storage and a thermal storage tank. When heating was needed in the cabin, the required heat was retrieved from the insulated storage tank. The analysis revealed that the thermal energy storage in the tank averaged 2.15 kW per day, with an energy efficiency of 83% [15].

Kaya et al. conducted theoretical and experimental research on a solar collector drying system with heat pipes and heat recovery. Experiments carried out in Karabuk climate conditions showed that at an average irradiance of 770 W/m^2, the temperature of the drying chamber was 49% higher than the ambient temperature. Furthermore, the average efficiency of the system was 24% [16].

Machine learning (ML) has recently become a useful technology that can develop high-accuracy models in various fields, especially data analysis. This technology works by mimicking the human brain's ability to discern patterns and establish relationships between input and output data without prior assumptions [17]. Artificial neural network models (ANNs) that mimic the functioning of the Human Brain can effectively predict PV parameters and optimize drying processes. Their ability to simulate process variables, self-tune, and improve performance for a specific task is promising. Additionally, machine learning can be used to better understand the drying processes of agricultural and industrial products and to model nonlinear processes. Machine learning algorithms have been used to eliminate the complexity in the drying process of various agricultural products such as banana [18], dragon fruit [19], and pumpkin [20]. When the literature was examined, studies emerged in which various mathematical and ML methods were used to examine solar drying systems. Some of these studies are highlighted below.

Saydam et al. conducted the design and experimental analysis of a SAC with a double-pass V-type absorber surface. An attempt was made to estimate the SAC exit temperature using three different artificial neural network algorithms. Their analysis revealed an average thermal efficiency of 56% with a maximum temperature difference of 36°C between the collector inlet and outlet. The best results among the ANN models were obtained using the Levenberg-Marquardt (LM) learning algorithm [21].

In another study, Özdemir et al. experimentally researched the convective infrared and heat recovery drying systems and modeled the results achieved using the Response Surface Methodology (RSM). In modeling, LM and Fermi transfer function algorithms estimate drying parameters such as moisture content and drying rate. Multiple coefficients of determination (R2), root mean square error (RMSE), and mean absolute percentage error (MAPE) were used in modeling for evaluation. Additionally, the energy efficiency of the system was found to be 18% on average [22].

Saydam et al. investigated the drying performance of a SAC in a drying chamber. In the test results, the average drying rate was found to be 0.0017 g water/g dry matter. The best results in mathematical modeling of drying rates were obtained with sigmoid and empirical Gaussian Process Regression (GPR) models [23].

Şevik et al. designed and tested a new mushroom drying system using an air heat pump and solar energy at different air flow rates. Moisture content and drying parameters obtained from this system were modeled using the Levenberg-Marquardt learning algorithm and ANN. R^2, MAPE, and RMSE were taken into account to determine the statistical validity and accuracy of the models. The study concluded that the experimental results were consistent with the modeling results [24].

In this study, unlike the literature, the performance of a novel solar energy-assisted drying system has been examined, focusing on the prediction of key parameters such as cabin temperature, moisture content, and overall efficiency using machine learning algorithms to enhance the effectiveness of drying systems. Drying of nettle products using a solar energy-assisted drying system was investigated. The system is designed to be used even on cloudy days in summer or in winter with low irradiance. Additionally, research on modeling the room temperature, total efficiency and moisture content values obtained from this system using machine learning algorithms is presented. The aim is to facilitate analysis by better understanding system dynamics and drying parameters.

II. Materials and Methods

A. Experimental System

Products were dried using airflow in a closed cabin that does not transmit solar radiation. The hot air for drying the products in the cabin was obtained from an SAC. Solar drying processes can be conducted during the summer when ambient temperatures and solar radiation are high. Therefore, experiments were conducted during the winter when ambient temperatures and solar radiation were lower. Additionally, photovoltaic panels were used in the design to meet the energy needs of electrical devices in the system. This allows the drying system to be used in areas without access to electricity.

The system was designed to operate during winter conditions as well, so concentrators were used to increase the amount of solar radiation. Figure 1 shows the schematic view of the drying system, while the front and rear views of the assembled system are presented in Figure 2. This system, which will be used in the drying of agricultural and industrial products, is an indirect drying system in which concentrated SAC and photovoltaic modules are combined. The hot air obtained from the air collector was conveyed to the drying cabin with the assistance of a fan. An automation system controlled the humidity and temperature of the drying cabin, while other sensor data from the system was also recorded in real time by the same automation system. Cooling with water was implemented to prevent overheating of the photovoltaic module, and the hot water obtained from this process was used to preheat the inlet air of the air collector. A heat exchanger was used for this preheating process. The electrical energy generated from the photovoltaic module was stored in a solar battery and later used to meet the electricity needs of the fan, pump, and automation system.

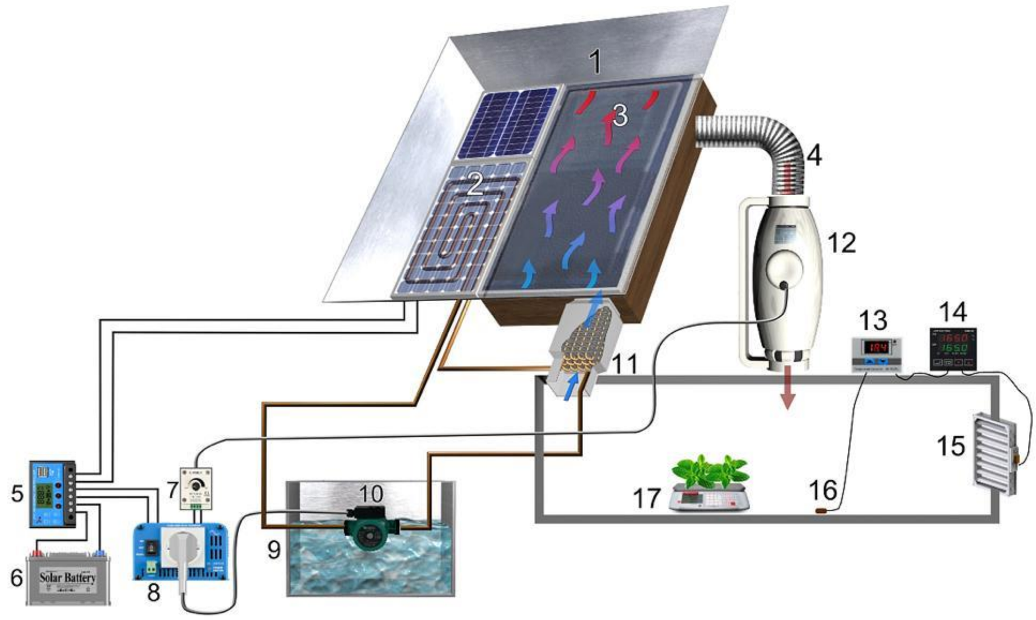

Figure 1. Appearance of the system

Figure 2. Indirect solar-powered drying system: (a) rear view, (b) front view

Table 1 presents the specifications of the measurement instruments used in the drying system.

Table 1. Technical Specifications of Measurement Instruments in the Experimental System

Equipment	Specifications
K-Type Thermocouple	K-type TP-01 Thermocouple Measurement Range: -50°C to 400°C
18b20 Temperature Probe	Waterproof 18b20 Temperature Probe Measurement Range: -20°C to 105°C
Hygrometer	Humidity: 0-100%RH ±3% (Max ±5%) RH
Solar Meter	PCE, 0–2000 W/m² ±5 W/m²

Multimeter	DC Voltage Range Resolution Accuracy: 200mV- 600V 1V: ± (0.5% 2) DC Current Range: 20uA-10A 10mA ± (1% 2)
Load Cell	Capacity: 0-5 kg ±0.002 kg Operating Temperature Range: -20/80°C

B. Artificial Neural Network Algorithm

ANNs are artificial intelligence models that mimic the functioning of the human brain. ANNs associate specific input values with output values based on given inputs [13]. ANNs have various applications, including pattern recognition, prediction, and classification, and are computer systems capable of performing human-like learning through their learning capabilities. This system consists of artificial neurons, and the weight value of each connection is where the information is stored. Training and testing data sets are typically used when creating an ANN model. These data sets are used during the model's learning process to evaluate its accuracy. ANNs, an important artificial intelligence technique, consist of three fundamental layers: the input, hidden, and output layers. Input data is directly applied to the input layer, so the number of neurons in the input layer is equal to the number of different input samples at any given time [25]. Then, these data go through operations such as summation, multiplication, and activation functions until they reach the output layer. Finally, the network is tested with test data that was not used during training, and its accuracy is determined. This study used a feedforward neural network as the learning function, and a backpropagation algorithm (multilayer perceptron) was used as the training function.

C. Artificial Neural Network Algorithm

Support Vector Machines, introduced by Boser and his colleagues, encompassed classification and non-linear function estimation, which attracted the interest of many researchers [26]. For regression, the support vector method is formulated as a convex optimization problem, particularly a second-order programming (QP) problem. To achieve this, the approximate problem is transformed into a constrained optimization problem by using Vapnik's ε-insensitive loss function [27]. Particularly, SVM models exhibit excellent scalability in high-dimensional input spaces. They find applications in engineering, time series analysis, handwriting recognition, face recognition, speaker identification, healthcare, and many other fields.

D. Artificial Neural Network Algorithm

The decision tree algorithm in ML is a method for the classification and prediction of non-linear functions based on a gradient-boosting technique [28]. Gradient Boosting Decision Trees (GBDT) consist of a series of weak classification models that have a strong relationship among them. The number of these weak classification models is repeated until it reaches a predetermined value, and a strong classification model is obtained by training the last weak classification model. The gradient boosting algorithm differs from the random forest algorithm. Additionally, the gradient boosting algorithm predicts the error of each weak classification algorithm and gradually reduces this error. Thus, a strong model is obtained through hundreds of iterations.

E. Comparison Statistical Metrics

Three fundamental measures have been considered when evaluating the results of ANNs, SVM, and GBDT algorithms. These measurements include determination coefficient (R^2), root mean squared error (RMSE), and mean absolute error (MAE). The detailed equations and explanations of these metrics are provided in Table 2. In Table 2, p_i, e_i, and n represent the prediction, experimental data, and number of observations, respectively.

Table 2. Comparison metrics

Metric	Equation	Description
R^2	$1 - \frac{\sum(e_i - p_i)^2}{\sum(e_i - e)^2}$	This metric provides information about how well a model can predict a particular measured dataset. The value of R^2 ranges from 0 to 1. As the R^2 value approaches 1, it indicates better performance [29].
RMSE	$\sqrt{\frac{1}{n}\sum_{i=1}^{n}(p_i - e_i)^2 \times 100}$	RMSE provides information about how well a model can predict a series of measured data. It exhibits better performance when RMSE is close to zero [30].
MAE	$\frac{1}{n}\sum_{i=1}^{n}\lvert e_i - p_i\rvert \times 100$	MAE evaluates the absolute magnitude of differences between corresponding data points and allows for a direct comparison between the predicted values and actual observations in a given context. A low MAE value indicates better prediction [13].

III. EXPERIMENTAL ANALYSIS

The electrical power gain generated from the PV/T module can be calculated as follows:

$$\dot{E}_{el} = V.I \qquad (1)$$

Where, V is the PV module voltage, and I is the current. PV module electrical efficiency can be found with Equation 2 below:

$$\eta_m = \frac{\dot{E}_{el}}{I(t)xA} \qquad (2)$$

Where, I(t) refer to the solar radiation intensity, and A refers to the PV module area. The total thermal efficiency of the drying system can be calculated using Equation 3 below:

$$\eta_{total} = \frac{\dot{Q}_{total}}{I(t)\times A_{sc} + \dot{W}_f + \dot{W}_p} \qquad (3)$$

The total thermal energy gain of the system can be calculated using Equation 4.

$$\dot{Q}_{total} = +\dot{Q}_{PV} + \dot{Q}_{COL} \qquad (4)$$

Thermal energy obtained from the PV module can be calculated by measuring the input water temperature and the exit water temperature [31].

$$\dot{Q}_{PV} = \dot{m}_w \times c_p \times (T_{PV,in} - T_{PV,out}) \qquad (5)$$

Thermal energy obtained from the air collector can be calculated with Equation 6 using the inlet and outlet air temperatures of the collector.

$$\dot{Q}_{SAC} = \dot{m}_{air} \times c_{p,air} \times \left(T_{SAC,out} - T_{SAC,in}\right) \tag{6}$$

Nettle moisture content values on a wet basis can be calculated using Equation 7:

$$MC = \frac{M_i - M_d}{M_d} \tag{7}$$

Where, M_i is the initial mass of the dried products and M_d is the mass of the product in the dried state.

IV. RESULT AND DISCUSSIONS

In this section, the performance of the solar energy-assisted drying system was evaluated using stinging nettles in October 2022. The system's design and installation were examined, and the obtained data during the drying process were evaluated to assess how successfully the drying process could be modeled using artificial neural network models.

The variation of ambient temperature and radiation intensity in the vicinity of the drying system is depicted in Figure 3. Throughout the study, data recorded at one-minute intervals were averaged over twelve-minute intervals to generate the graphs. The experiment, commencing at 11:00, saw the ambient temperature starting at 33.3 °C and reaching a peak of 53 °C. The average ambient temperature was calculated to be 42.8 °C. The right axis of the same graph displays the intensified radiation data. The radiation intensity peaked at 14:00 and then began to decrease. The highest radiation intensity recorded was 1013 W/m^2, while the average solar radiation intensity was found to be 795 W/m^2.

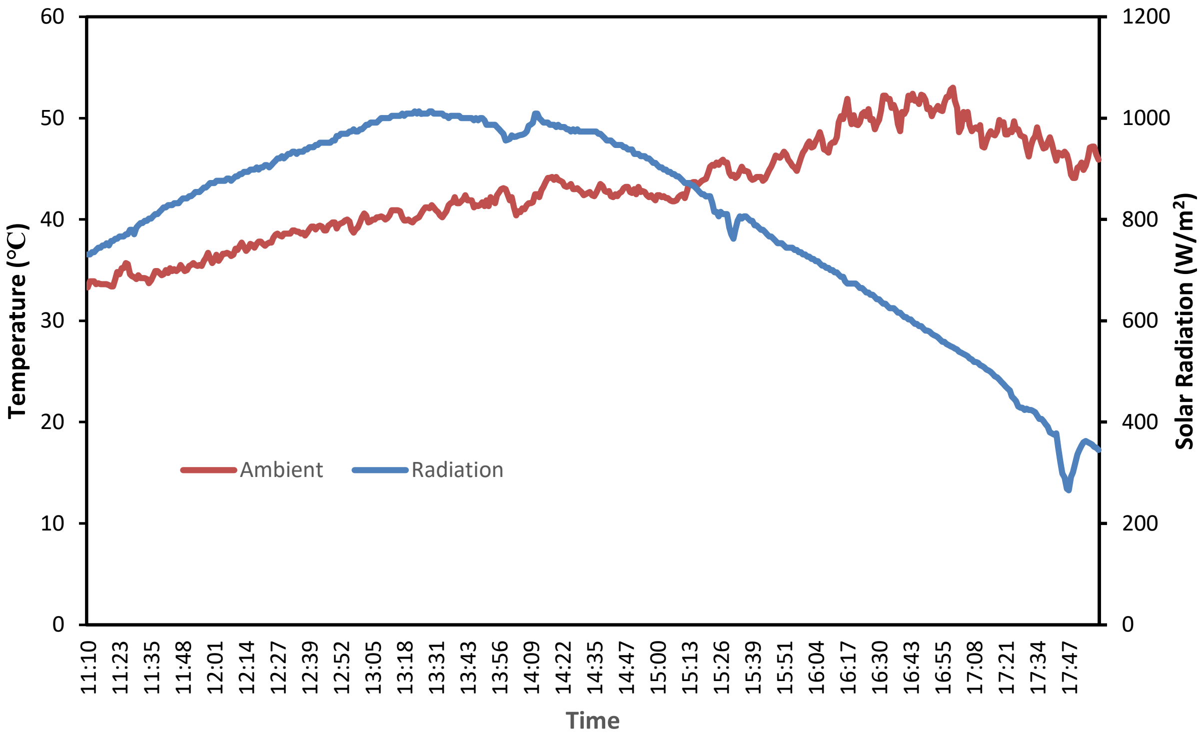

Figure 3. Change of radiation with environmental temperature.

Figure 4 shows the variation in drying chamber temperature, photovoltaic module rear temperature, and ambient temperature. Throughout the day, the temperature of the photovoltaic panel ranged from a minimum of 38°C to a maximum of 52°C. The average rear temperature of the photovoltaic module was calculated at 43°C. Despite fluctuations in the rear temperature of the photovoltaic module during the experiment, the cooling process occurred. The drying cabin temperature was determined to be an average of 55.5°C during the drying process. Observations showed that it reached a minimum of 35°C and a maximum of 62°C. This drying chamber temperature facilitated the drying of the nettle.

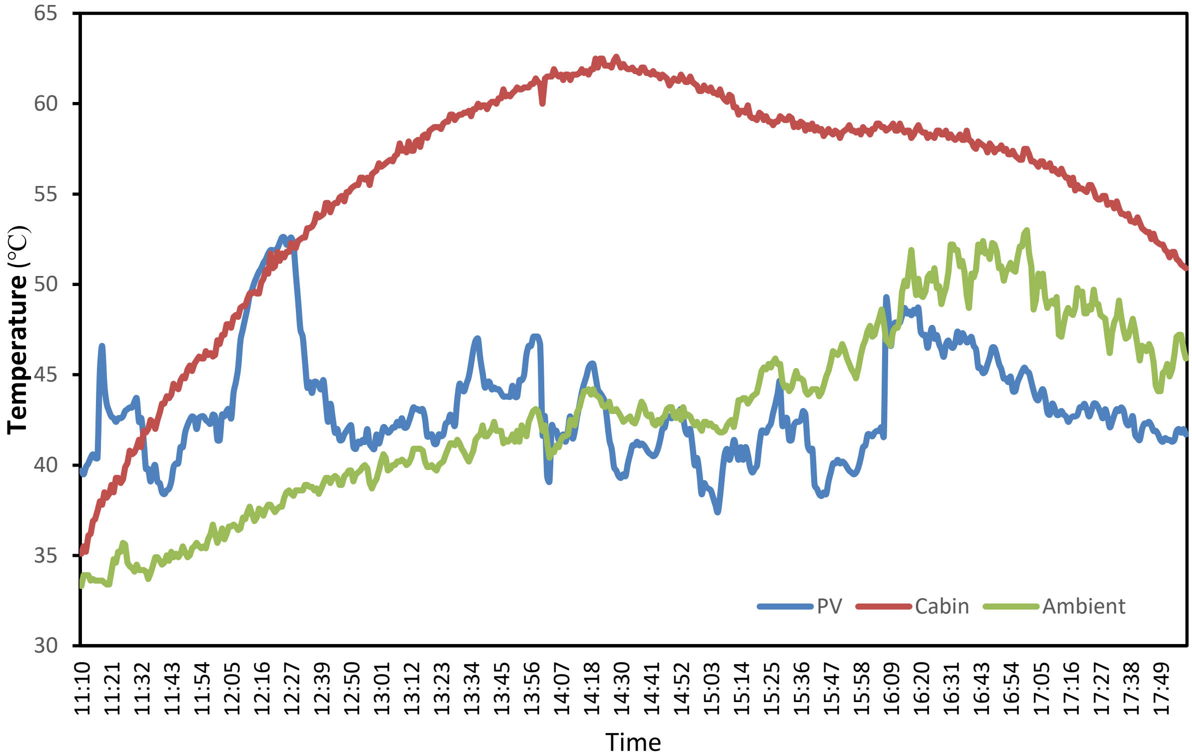

Figure 4. Change of drying cabin temperature, photovoltaic module rear temperature and ambient temperature

Figure 5 shows the heat obtained from the SAC, the heat obtained from the PV module, and the heat transferred to the drying chamber. The average thermal energy obtained from the collector was calculated as 119 W, while the thermal energy obtained from the PV module was 35 W. The thermal energy transferred to the drying chamber was found to be 154 W. While the collector provided 77% of the thermal energy used in the drying process, the remaining 23% was obtained from the PV model. Thus, cooling is provided in the PV module, and additional thermal energy is used for drying.

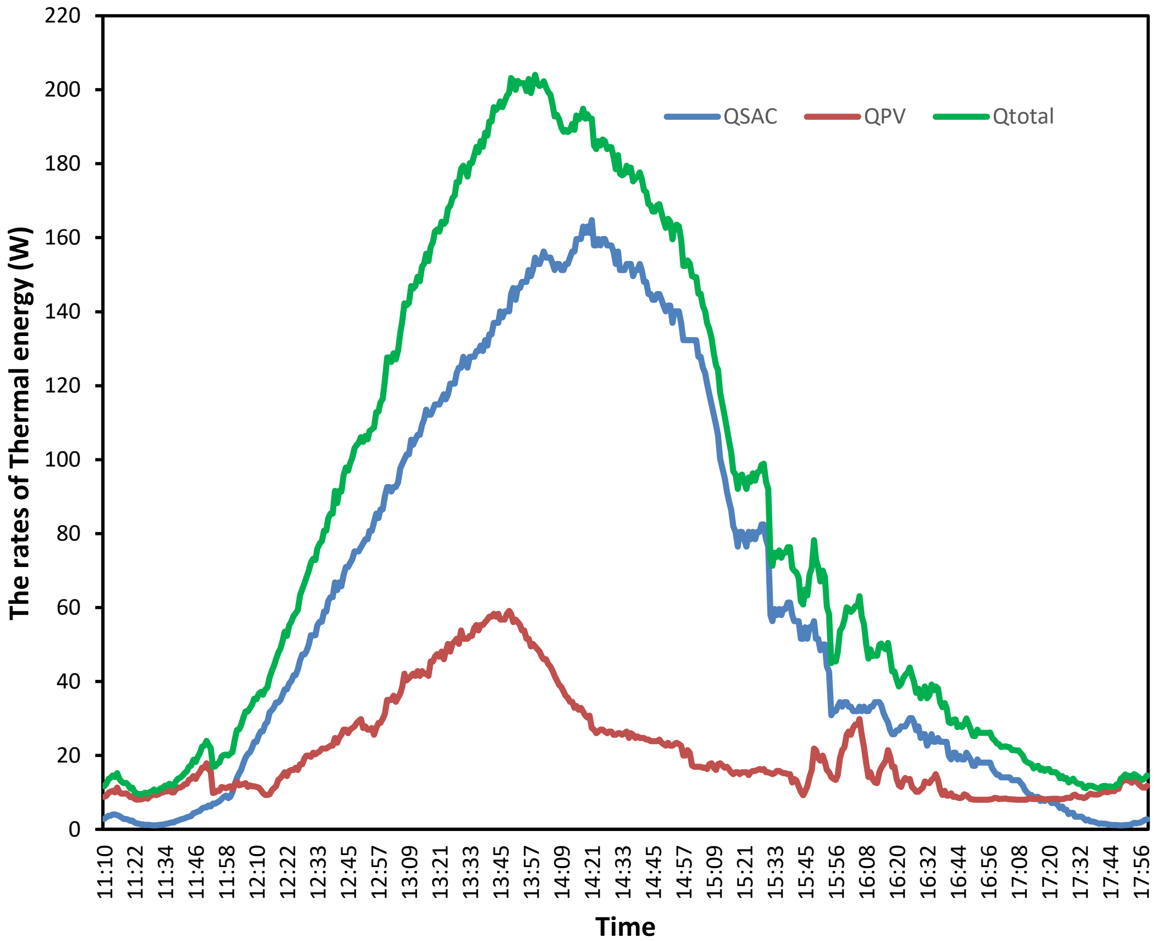

Figure 5. SAC, PV/T and drying cabin thermal energy flows

The variation in total efficiency during the experiment is shown in Figure 6. Total efficiency is expressed as the ratio of the thermal energy transferred to the drying chamber to the solar radiation intensity incident on the experimental system, as indicated in Equation 3. At the beginning of the experiment, the total efficiency was approximately 3.5%, and it increased as the solar radiation intensity increased. The total efficiency reached its highest value of 37%. Subsequently, as the solar radiation intensity decreased, the total efficiency also decreased. The average total efficiency was calculated as 16.8%.

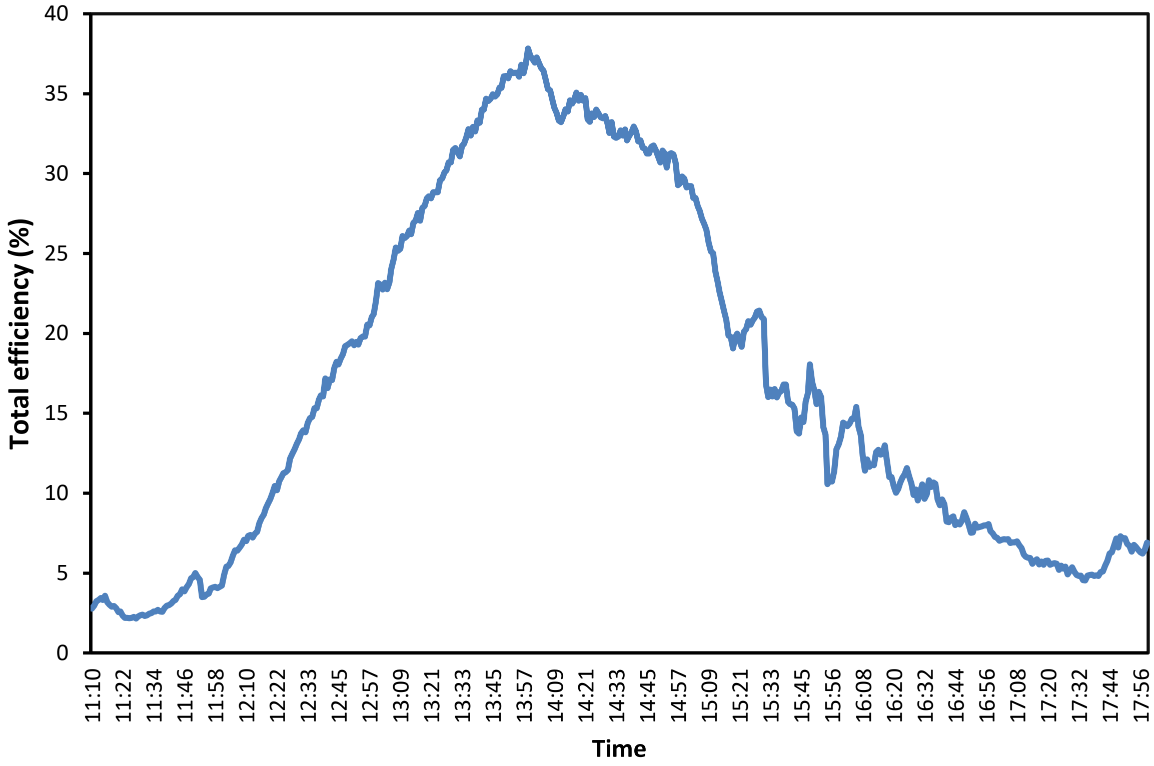

Figure 6. Change in total efficiency during the experiment

Figure 7 shows the change in the nettle's moisture content during the experiment. The nettle was dried from a moisture content of 11.18 g water / g dry matter to 1.18 g water / g dry matter.

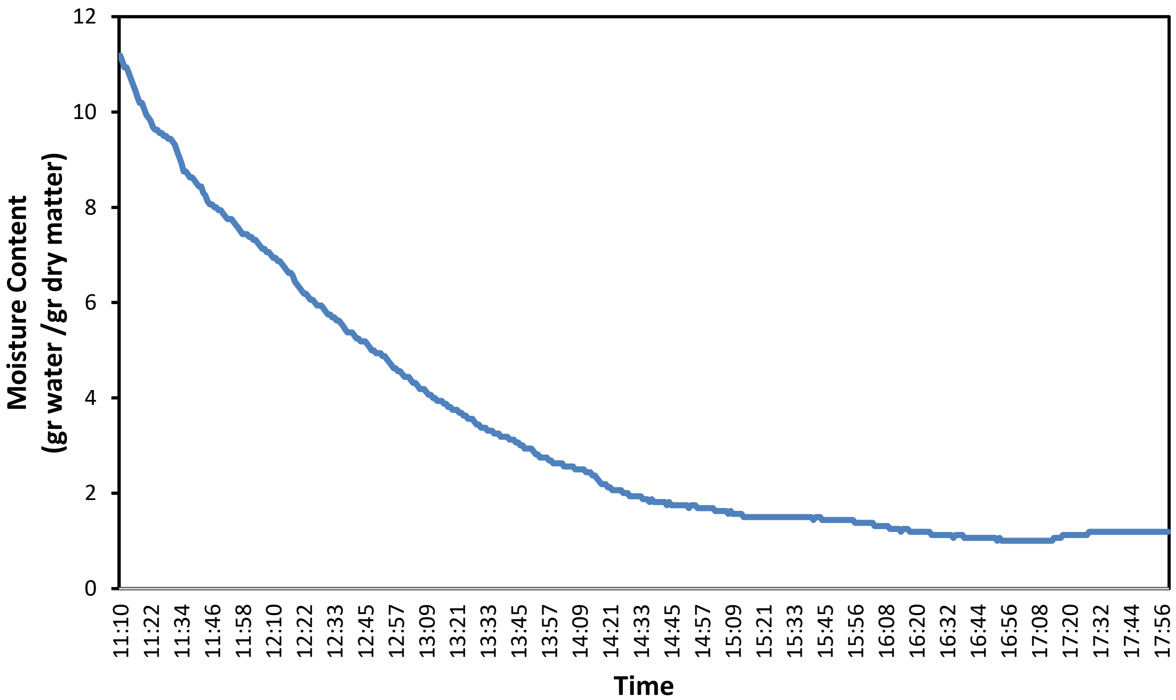

Figure 7. Moisture content change during the experiment

A. EVALUATING AND COMPARING PREDICTION RESULTS

The experimental dataset was divided into two parts, with 60% used for training and 40% for testing. The data was split using random sampling. The input data for the specified prediction values is introduced in the relevant sections of the following graphics. The data obtained from ANN, support vector machines, and gradient-boosting decision tree ML algorithms are presented in Table 3.

Table 3. Statistical metric comparison of machine learning algorithms

Label	Statistical Metrics	ANN	SVM	GBDT
Cabinet Temperature	R^2	0.94	0.98	0.95
	RMSE, %	40.30	13.31	17.20
	MAE, %	31.50	9.015	13.10
Moisture Content	R^2	0.95	0.99	0.99
	RMSE, %	15.96	5.40	6.91
	MAE, %	12.35	3.86	5.05
Total efficiency	R^2	0.94	0.99	0.97
	RMSE, %	35.20	4.60	39.30
	MAE, %	26.10	3.60	29.20

According to the statistical metrics shown in Table 3, the SVM algorithm has demonstrated a significant superiority in predicting the cabin temperature. The SVM algorithm has outperformed the ANN and GBDT algorithms in all metrics. Again, the best results are obtained with the SVM algorithm across all statistical metrics when predicting humidity content. Following the SVM algorithm, the GBDT algorithm and the ANN algorithm have succeeded. Although the GBDT algorithm did not perform as well as the SVM algorithm in predicting humidity content, it still yielded successful results. Finally, looking at the prediction of total efficiency, the SVM algorithm has shown a significant superiority over the other two algorithms according to the statistical metrics. While all three ML algorithms perform well according to the R^2 statistical metric, other statistical metrics reveal their fundamental differences. Despite the instantaneous changes in test values, the SVM algorithm has been able to predict them quite well.

Figure 8 shows the variation in predicted cabin temperature values using the YSA, SVM, and GBDT algorithms based on the data obtained from the experimental system. Time, PV module rear temperature, collector output temperature, PV/T output temperature, and solar radiation data were provided as inputs to the ML algorithms to predict the cabin temperature. When Table 3 and Figure 8 are considered together, it is observed that the SVM algorithm is the most successful in predicting cabin temperature. Additionally, it is seen that the GBDT algorithm is also quite successful, but it falls behind the SVM algorithm in some observation values.

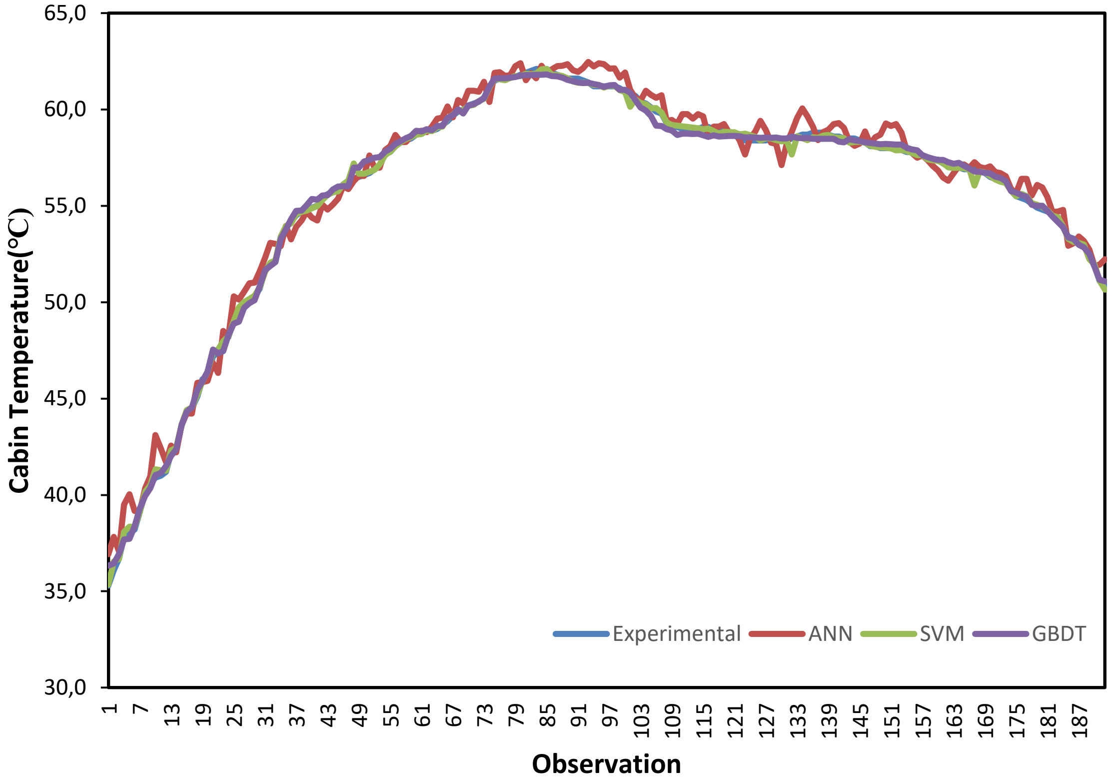

Figure 8. Graph of cabin temperature according to machine learning algorithms predictions

Figure 9 shows the variation in predicted moisture content values according to the YSA, SVM, and GBDT ML algorithms. Time, PV module rear temperature, cabin temperature, solar radiation, and ambient temperature data were provided as inputs to the ML algorithms to predict the moisture content. Based on the statistical metrics in Table 3 and the data in Figure 9, it was found that the most successful predictions were obtained from the SVM algorithm using the experimental system's measured data. The GBDT algorithm also made successful predictions, but errors in predicting actual data at the beginning of the experiment were observed. The YSA algorithm's significant errors in predictions towards the end of the experiment negatively affected its performance.

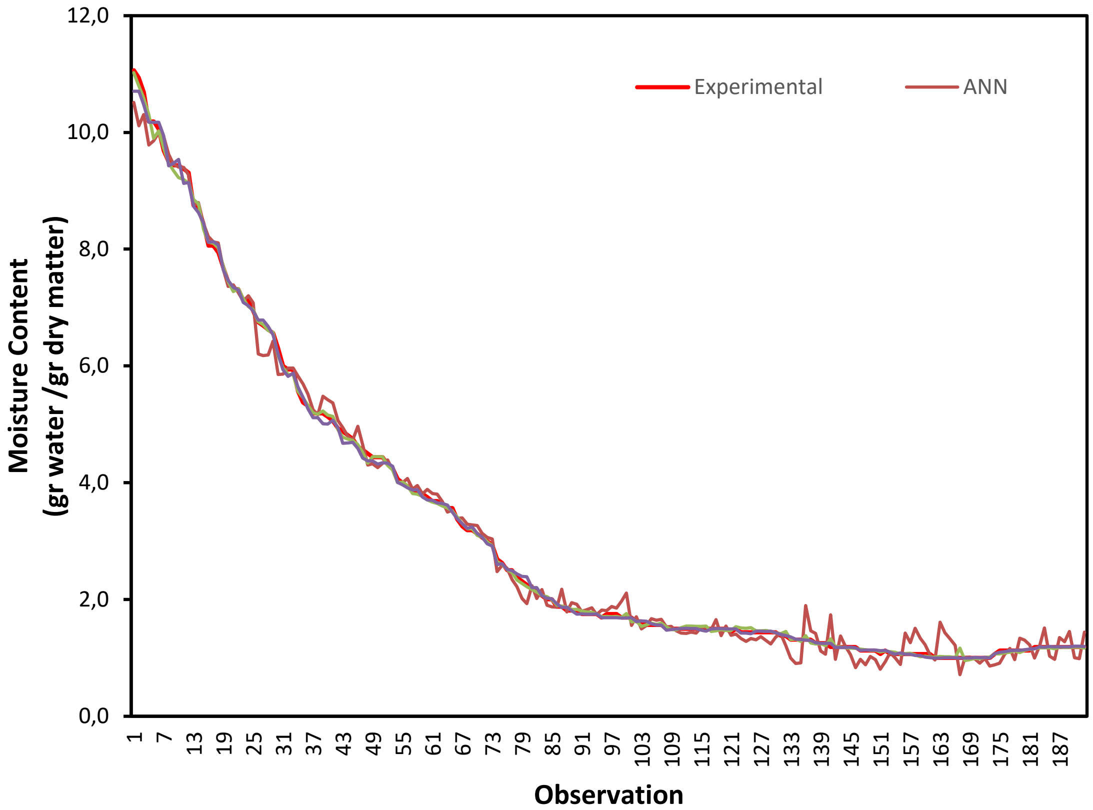

Figure 9. Graph of moisture content according to machine learning algorithms predictions

The graph in Figure 10 illustrates the variation in total efficiency predicted by ML algorithms. Time, FV module input-output temperatures, collector input-output temperatures, cabin temperature, solar radiation intensity, and ambient temperature data were inputs to the ML algorithms to predict total efficiency. As seen in the statistical metrics in Table 3 and Figure 10, the SVM algorithm best predicted the total efficiency results from the data obtained from the experimental system. Although the YSA and GBDT algorithms made fairly close predictions, they lagged behind the SVM algorithm.

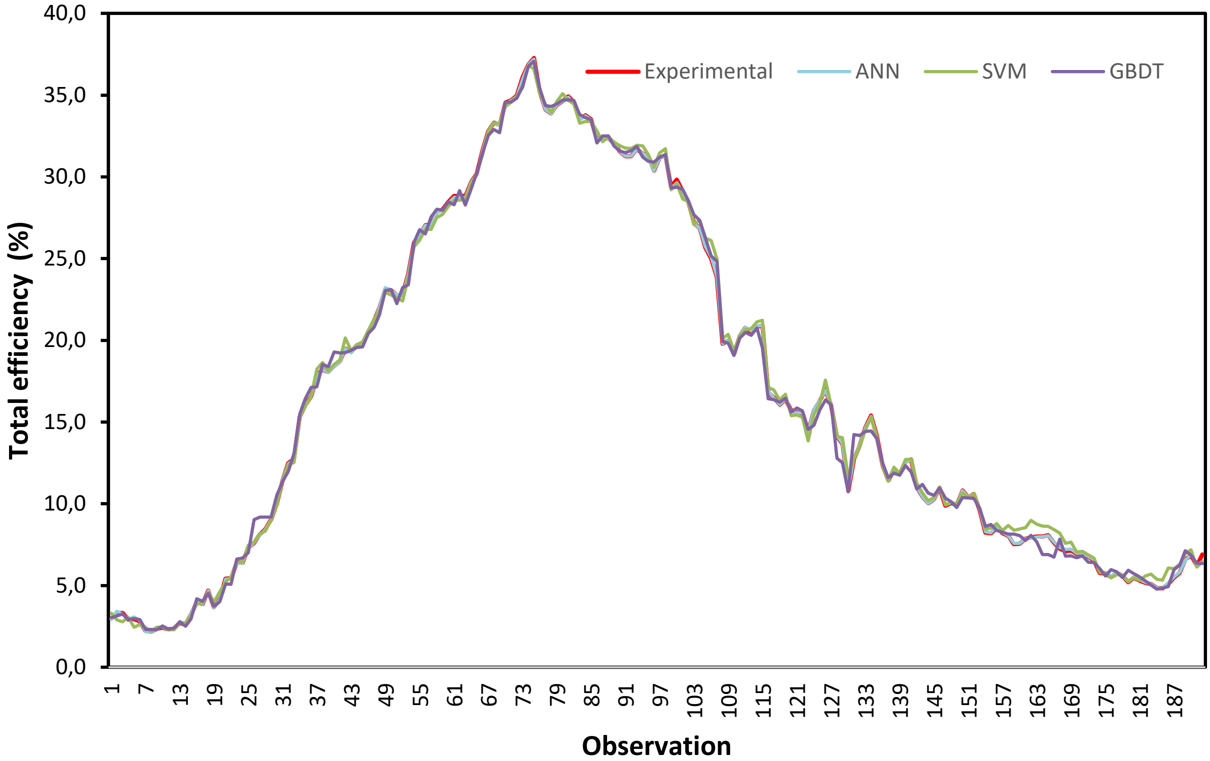

Figure 10. Graph of total efficiency according to machine learning algorithms predictions

V. CONCLUSION

In this study, the performance of a novel solar energy-assisted drying system has been examined, focusing on predicting key parameters such as cabin temperature, moisture content, and overall efficiency using machine learning algorithms to enhance the effectiveness of drying systems. The system utilized thermal energy obtained from a SAC and a PV/T to dry stinging nettle. The findings obtained during the experiment are summarized below:

- The average solar irradiance was 795 W/m^2, while the average ambient temperature was calculated to be 42.8 °C during the experiment.
- Throughout the experiment, the average rear temperature of the PV module was calculated to be 43 °C. Additionally, the PV rear temperature ranged from a minimum of 38 °C to a maximum of 52 °C during the day.
- The average cabin temperature was determined to be 55.5 °C, with observed fluctuations between 35 °C and 62 °C.
- The average thermal energy transferred to the drying cabin was calculated as 154 W, with 77% of this energy sourced from the collector and the remaining 23% from the PV module.
- The total efficiency of the drying system was calculated at a maximum of 37%, with an average total efficiency of 16.8%.
- The SVM algorithm provided the best predictions in cabin temperature prediction, with R^2, RMSE, and MAE statistical metric values of 0.98, 13.31%, and 9.015%, respectively.
- For the prediction of moisture content, the SVM algorithm achieved the best results with R^2 of 0.99, RMSE of 5.4%, and MAE of 3.86%.
- According to statistical metrics and the obtained prediction values, the SVM algorithm significantly outperformed others in predicting the total efficiency.
- The SVM machine learning emerged as the best prediction algorithm compared to YSA and GBDT algorithms.

V. REFERENCES

[1] M. Aktaş, A. Khanlari, A. Amini, and S. Şevik, 'Performance analysis of heat pump and infrared–heat pump drying of grated carrot using energy-exergy methodology', *Energy Conversion and Management*, vol. 132, pp. 327–338, Jan. 2017.

[2] M. S. Buker and S. B. Riffat, 'Solar assisted heat pump systems for low temperature water heating applications: A systematic review', *Renewable and Sustainable Energy Reviews*, vol. 55, pp. 399–413, Mar. 2016.

[3] M. O. Karaağaç, A. Ergün, A. Etem Gürel, İ. Ceylan, and G. Yıldız, 'Assessment of a novel defrost method for PV/T system assisted sustainable refrigeration system', *Energy Conversion and Management*, vol. 267, p. 115943, Sep. 2022.

[4] İ. Arslan, 'Tekirdağ koşullarında polikristal ve monokristal tip pv güneş panellerinin verimlilik karşılaştırılması', *Monocyrstal and polycrystal solar panels under tekirdag conditions investigation of efficiency*, 2018, Accessed: Feb. 23, 2021.

[5] M. O. Karaagac, H. Oğul, and F. Bulut, 'Sinop İli Koşullarında Monokristal ve Polikristal Fotovoltaik Panellerin Değerlendirilmesi', *Türk Doğa ve Fen Dergisi*, vol. 10, no. 1, Art. no. 1, Jun. 2021.

[6] M. Abdelgaied, A. S. Abdullah, A. E. Kabeel, and H. F. Abosheiasha, 'Assessment of an innovative hybrid system of PVT-driven RO desalination unit integrated with solar dish concentrator as preheating unit', *Energy Conversion and Management*, vol. 258, p. 115558, Apr. 2022.

[7] M. Abderrahman, B. Abdelaziz, and O. Abdelkader, 'Thermal performances and kinetics analyses of greenhouse hybrid drying of two-phase olive pomace: Effect of thin layer thickness', *Renewable Energy*, vol. 199, pp. 407–418, Nov. 2022.

[8] F. Durmaz, R. C. Akdeniz, and F. Kömekçi, 'Fotovoltaik Enerji ile Tarımsal İşletmelerin Enerji Gereksiniminin Karşılanabilirliği: Manisa - Turgutlu Örneği', *TMBD*, vol. 13, no. 3, Art. no. 3, Dec. 2017.

[9] E. K. Akpinar, 'Drying of mint leaves in a solar dryer and under open sun: Modelling, performance analyses', *Energy Conversion and Management*, vol. 51, no. 12, pp. 2407–2418, Dec. 2010.

[10] M. Aktaş, İ. Ceylan, A. Ergün, A. E. Gürel, and M. Atar, 'Assessment of a solar-assisted infrared timber drying system', *Environmental Progress & Sustainable Energy*, vol. 36, no. 6, pp. 1875–1881, 2017.

[11] I. Ceylan and A. Ergun, 'Psychrometric analysis of a timber dryer', *Case Studies in Thermal Engineering*, vol. 2, pp. 29–35, Mar. 2014.

[12] Ö. Demir, 'Kızılötesi Kurutucuda Nane Bitkisinin Optimum Kurutma Sıcaklığının Belirlenmesi', *Bitlis Eren Üniversitesi Fen Bilimleri Dergisi*, vol. 8, no. 3, Art. no. 3, Sep. 2019.

[13] M. O. Karaağaç, A. Ergün, Ü. Ağbulut, A. E. Gürel, and İ. Ceylan, 'Experimental analysis of CPV/T solar dryer with nano-enhanced PCM and prediction of drying parameters using ANN and SVM algorithms', *Solar Energy*, vol. 218, pp. 57–67, Apr. 2021.

[14] İ. Ceylan, M. Aktaş, and H. Doğan, 'Güneş Enerjili Kurutma Fırınında Elma Kurutulması', *Politeknik Dergisi*, vol. 9, no. 4, Art. no. 4, Dec. 2006.

[15] A. Uçar and A. Oral, 'Havalı Güneş Kollektörlü Bir Isıtma Sisteminin Deneysel Olarak İncelenmesi', *International Journal of Pure and Applied Sciences*, vol. 9, no. 2, Art. no. 2, Dec. 2023.

[16] E. Kaya, H. Dumrul, and S. Yilmaz, 'Isı Borulu Güneş Kollektörlü Kurutma Sisteminin Tasarımı ve Deneysel Analizi', *Politeknik Dergisi*, vol. 26, no. 2, Art. no. 2, Jul. 2023.

[17] S. M. Mousavifard, M. M. Attar, A. Ghanbari, and M. Dadgar, 'Application of artificial neural network and adaptive neuro-fuzzy inference system to investigate corrosion rate of zirconium-based nano-ceramic layer on galvanized steel in 3.5% NaCl solution', *Journal of Alloys and Compounds*, vol. 639, pp. 315–324, Aug. 2015.

[18] A. K. Yıldız, H. Polatcı, and U. Harun, 'Farklı Kurutma Şartlarında Muz (Musa cavendishii) Meyvesinin Kurutulması ve Kurutma Kinetiğinin Yapay Sinir Ağları ile Modellenmesi', *Tarım Makinaları Bilimi Dergisi*, vol. 11, no. 2, pp. 173–178, 2015.

[19] G. V. S. Bhagya Raj and K. K. Dash, 'Microwave vacuum drying of dragon fruit slice: Artificial neural network modelling, genetic algorithm optimization, and kinetics study', *Computers and Electronics in Agriculture*, vol. 178, p. 105814, Nov. 2020.

[20] H. N. Bulus, A. Moralar, and S. Celen, 'Modeling the Moisture Content and Drying Rate of Zucchini (Cucurbita pepo L.) in a Solar Hybrid Dryer Using ANN and ANFIS Methods', *The Philippine Agricultural Scientist*, vol. 106, no. 3, Sep. 2023.

[21] D. B. Saydam, K. N. Çerçi, and E. Hürdoğan, 'V Tipi Havali Bir Güneş Kolektörünün Isil Performansinin Deneysel Olarak İncelenmesi Ve Yapay Sinir Ağlari İle Modellenmesi', *MBTD*, vol. 9, no. 4, Art. no. 4, Dec. 2021.

[22] T. Menlik, M. B. Özdemir, and V. Kirmaci, 'Determination of freeze-drying behaviors of apples by artificial neural network', *Expert Systems with Applications*, vol. 37, no. 12, pp. 7669–7677, Dec. 2010.

[23] D. B. Saydam, K. N. Çerçi, and E. Hürdoğan, 'Güneş Enerjili Yeni Tip Bir Kurutucuda Granny Smith Elmanın Kuruma Davranışının İncelenmesi', *Afyon Kocatepe Üniversitesi Fen Ve Mühendislik Bilimleri Dergisi*, vol. 21, no. 4, Art. no. 4, Aug. 2021.

[24] Ş. Seyfi; Aktaş, 'Güneş destekli ısı pompalı bir kurutucuda mantarın kuruma davranışlarının yapay sinir ağı kullanılarak modellenmesi', *Tarım Bilimleri Dergisi*, vol. 20, no. 2, pp. 187–202, 2014.

[25] A. Ergün, İ. Ceylan, B. Acar, and H. Erkaymaz, 'Energy–exergy–ANN analyses of solar-assisted fluidized bed dryer', *Drying Technology*, vol. 35, no. 14, pp. 1711–1720, Oct. 2017.

[26] B. E. Boser, I. M. Guyon, and V. N. Vapnik, 'A training algorithm for optimal margin classifiers', presented at the Proceedings of the fifth annual workshop on Computational learning theory, 1992, pp. 144–152.

[27] G.-Q. Lin, L.-L. Li, M.-L. Tseng, H.-M. Liu, D.-D. Yuan, and R. R. Tan, 'An improved moth-flame optimization algorithm for support vector machine prediction of photovoltaic power generation', *Journal of Cleaner Production*, vol. 253, p. 119966, Apr. 2020.

[28] T. Zhang, Y. Huang, H. Liao, and Y. Liang, 'A hybrid electric vehicle load classification and forecasting approach based on GBDT algorithm and temporal convolutional network', *Applied Energy*, vol. 351, p. 121768, Dec. 2023.

[29] S. G. Gouda, Z. Hussein, S. Luo, and Q. Yuan, 'Model selection for accurate daily global solar radiation prediction in China', *Journal of Cleaner Production*, vol. 221, pp. 132–144, Jun. 2019.

[30] D. S. K. Karunasingha, 'Root mean square error or mean absolute error? Use their ratio as well', *Information Sciences*, vol. 585, pp. 609–629, Mar. 2022.

[31] M. O. Karaağaç, A. Kabul, and H. Oğul, 'First- and second-law thermodynamic analyses of a combined natural gas cycle power plant: Sankey and Grossman diagrams', *Turk J Phys*, vol. 43, no. 1, pp. 93–108, Feb. 2019.